

Design of Barker code generator in optical domain using Mach-Zehnder interferometer

Rajiv Kumar^{1*}, Niranjana Kumar², Poonam Singh³

¹EEE Department NIT Jamshedpur, Jharkhand, India.

²EEE Department NIT Jamshedpur, Jharkhand, India.

³ECE Department NIT Rourkela, Odisha, India.

Abstract

We present a Barker code generator in optical domain for fiber-based and free space optical communication. It incorporates multiple Mach-Zehnder interferometer structures to generate the barker code in the optical domain. Electronics circuits have practical limitations on the speed of operation at the frequency higher than 10^{10} Hz. All-optical circuits can work at high frequency. It includes some considerable advantages of optical communication e. g. Compact size, immunity to electromagnetic interference, low attenuation, higher bandwidth and cheap computing. The paper describes the mathematical aspects of the proposed devices along with the appropriate layout diagram. The match between the analytical result and the MATLAB simulated result confirms the accuracy of the designed device.

Keywords- Barker code, Mach-Zehnder interferometer, Optical Communication.

I. INTRODUCTION

The rapid increasing demand for bandwidth has forced us to think about an alternative to the radio frequency (RF) Communication, Optical wireless communication (OWC) or free space optical communication (FSO) is becoming a good alternative to the RF Communication. OWC has several advantages it can support a data rate up to gigabits per second, low installation cost, narrow beam, robustness to electromagnetic interference. Several research works have been reported on FSO communication and researchers are continuously working to design the devices to support the FSO. The Various modulation scheme is implemented in optical domain using MZI, phase shift keyed [1], NRZ and RZ [2-3]. Optical signal processing can be done using MZI as a switch [4]. All-optical time division multiplexing switch is proposed [5]. Mach-Zehnder Interferometer is the best solution for long distance (>500m), high data rate (>28Gb/s) optical communications[6], all-optical logic XOR is demonstrated

experimentally at 20 and 40 Gb/s with the scheme demonstrated [7], In this paper a new scheme of all-optical programmable logic device (PLD) is proposed and described.[8], An all-optical multi-wavelength converter using a semiconductor optical amplifier based Mach-Zehnder interferometer is proposed and demonstrated[9], all-optical 3R burst mode receiver circuit operating with 40 Gb/s asynchronous, variable length bursts with intense power variation is proposed[10]. The switching activity of MZI can be used to implement various optical devices. The concepts of signal selectivity in the form of 1×4 optical signal router are discussed in [11]. Similarly, many researchers have employed the optical interferometer circuits, which is composed of optical couplers and optical delay devices, which are the basic element employed in various optical devices [12]-[14]. On the basis of the electro-optic effect and proper feedback mechanism, the optical clocked D flip-flop, optical shift register, and ripple counter are designed [15]. Using the concept of linear electro-optic effect, some work has been carried out to observe several combinational logical phenomena. Using the concept of pockel effect the concept associated with XOR/XNOR and AND logic gate [16], optical gray code converter and even parity checker [17], optical full-adder and full Sub-tractor [18].

The proposed paper describes the design of Barker code sequence generator using MZI and is structured as follows. In section 1, we have introduced the relevant research work carried out in the field of the free space optical communication, optical logic functionality, and optical switching systems. Section 2 presents the concept of the electro-optic effect and the implementation of optical clocked D flip-flop. Section 3 includes the designed detailed description of 5-Bit Barker code sequence generator using electro-optic effect-based Mach-Zehnder interferometer structure. Finally, section 4 represents the relevant conclusion.

II. ELECTRO-OPTIC EFFECT AND EO EFFECT BASED MZI STRUCTURE AND OPTICAL CLOCKED D FLIP USING THE MZI STRUCTURE

There are some specific types of material, whose refractive index changes with the application of electric field. Lithium niobat, Gallium Arsenide are some important electro-optic material. Basically, the Change in the refractive-index given by Eq. (1);

$$\Delta n = \left(\frac{n^3}{2} \right) rE \quad (1)$$

Where, r is electro-optic coefficient, and E is the electric field. We have certain materials, whose dielectric constant can be changed by the application of an electric field or magnetic field. Now, we can write the phase changes using the Eq. (2)

$$\Delta\phi = \frac{2\pi}{\lambda} (\Delta n)L \quad (2)$$

Now, from Eq. (1), we can write

$$\Delta\phi = \frac{2\pi}{\lambda} \left(\left(\frac{n^3}{2} \right) rE \right) L \quad (3)$$

Let us say, if the voltage difference between these two electrodes is V and d is the separation between the electrode, the electric field will be approximately V/d . Hence, we can write;

$$\Delta\phi = \frac{2\pi}{\lambda} \left(\left(\frac{n^3}{2} \right) \frac{V}{d} r \right) L \tag{4}$$

So, when no voltage is applied $\Delta\phi$ remains zero, and we apply the voltage (V) the phase must change by π . This particular voltage is known as the V_π . Hence, we can write

$$V_\pi = \frac{\lambda}{n^3} \frac{1}{r} \frac{d}{L} \tag{5}$$

The Mach-Zehnder interferometers (MZIs) can be used to perform the optical switching based on the principle of electro-optic (EO) effect. The channel waveguide can be created on the lithium-niobate substrate. The device contains two input ports and two output ports associated with electrodes. Hence, the refractive index of one of the arms of the MZI can be changed depending upon the voltage applied across one of the arms. The optical signal can be applied to the input port, and in the meanwhile, the light signal can be divided equally into two parts. Then this equally divided signal propagates through the two arms and again the signal combines and finally by a series of combination and distribution of signals, the output is observed at the two ports. Now, by putting the electrodes around the arms of the MZI, a kind of phase modulator can be created.

Table 1: Truth table of D-flip flop

Clock Signal	D	Q_n
0	x	Q_{n-1} (last state)
1	0	0
1	1	1

The MZI structure can be used to implement the optical clocked D flip-flop. As we know that the D flip-flop remains transparent, as the clock signal is high. The basic truth table can be represented using the table 1.

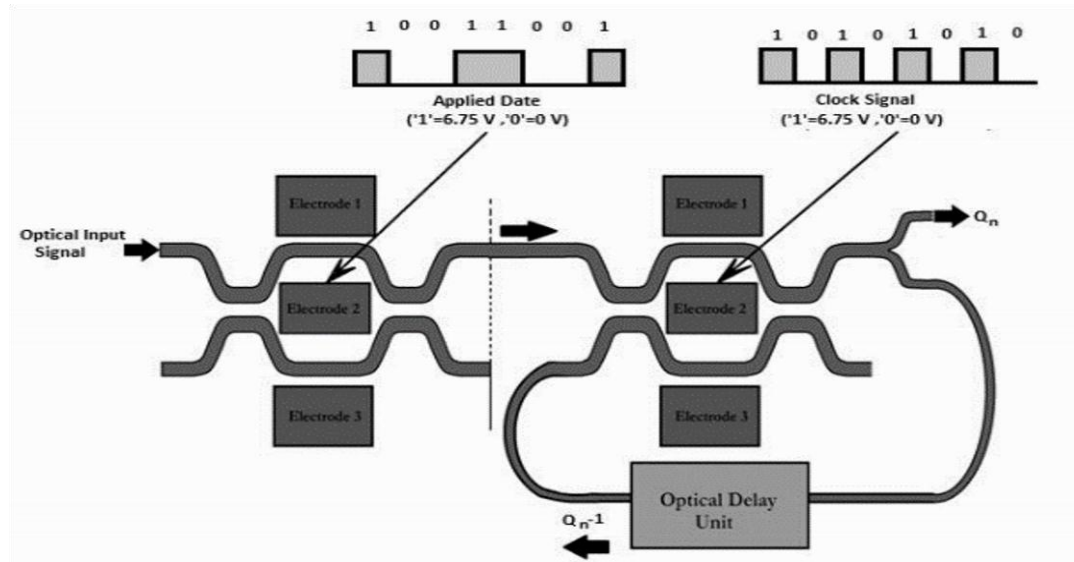


Fig 1: The Layout diagram of optical clocked D-flip flop

Figure 1 shows the layout diagram of the optically clocked D Flip-Flop. The first MZI can be used to convert the data bit in the optical domain. The second MZI is associated with feedback mechanism and an appropriate 1-bit optical delay unit. The optical equivalent of data bit obtained from the throughput output port of first MZI behaves as the optical input for the feedback assisted second MZI.

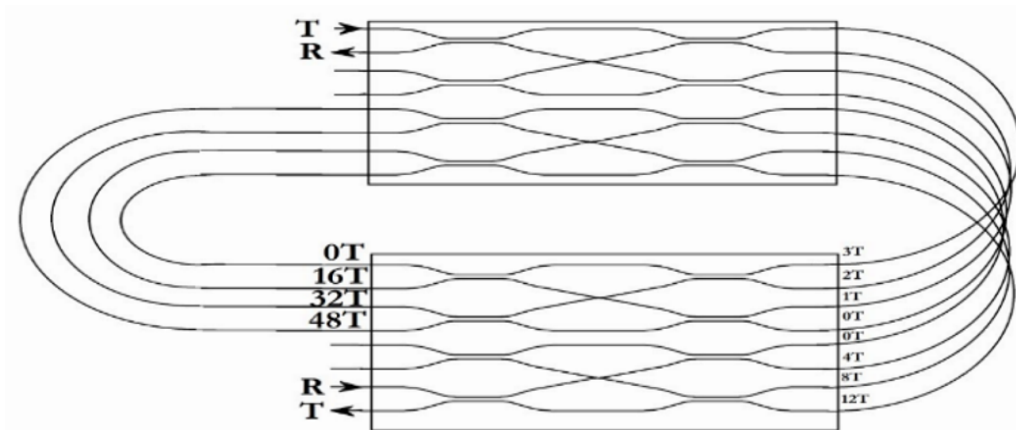


Fig 2: 1- bit optical delay unit

Fig. 2 shows the optical delay unit, composed of the complex architecture of loops of optical fiber which can be used to implement the MZI based optical clocked D flip-flop. The layout can be used for the numbers of a signal processing system such as short-term memory; packet switching network requires variable delays for queuing and packet retiming. The delay unit consists of 2-lithium niobate die each comprise of two 4×4

networks constructed by four directional couplers. The device operates at the wavelength $1.3 \mu m$. The directional coupler is controlled by bias electrode and single switching voltage. The 4×4 switch device is connected by suitable lengths of fibers that provide the delay in the multiple of $44 ps$. The two dice and twelve fiber loops are enclosed as an entity, which provides the physical strengths. The end faces of each die are anti-reflected, coated to suppress the interface reflection. The four input/output fibers are terminated with keyed connectors. The detailed mathematical analysis of optical clocked D flip-flop shows output power using Eq. (6) [15].

$$|Q_n|^2 = \sin^2\left(\frac{\Delta\varphi}{2}\right)|D_n|^2 + \cos^2\left(\frac{\Delta\varphi}{2}\right)|Q_{n-1}|^2 + |D_n||Q_{n-1}|\sin\Delta\varphi \tag{6}$$

Eq. (6) represents the expression of the output optical signal obtained from the D-flip flop. Where $\Delta\varphi = \frac{\pi}{v\pi}(clock - signal)$. The MATLAB simulation result has been generated. The MATLAB simulation result can be represented using the fig. 3.

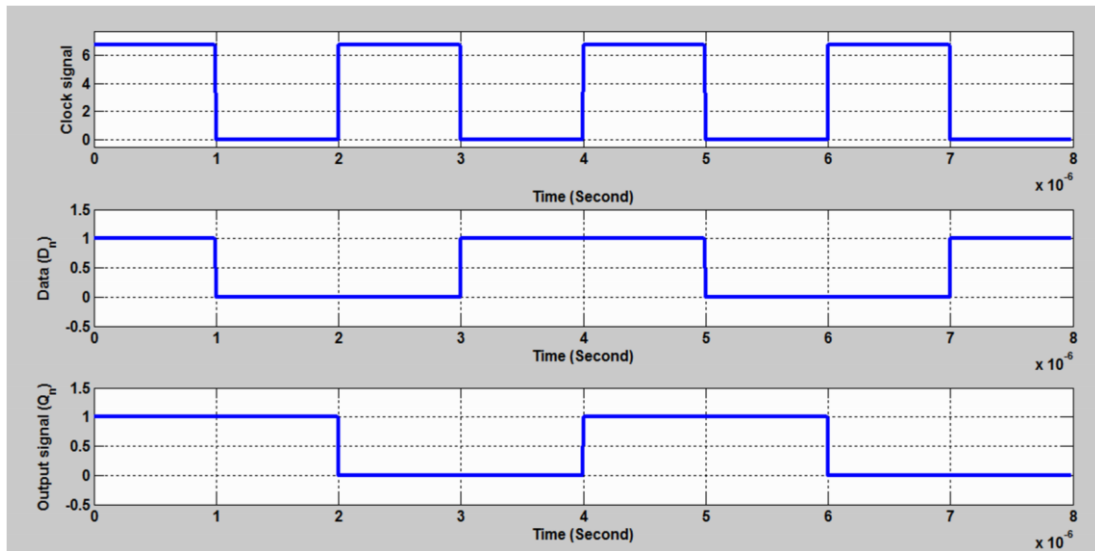


Fig. 3: MATLAB Simulation result of the proposed optical clocked D flip-flop

The simulation result can be verified by the table 1. However, the equivalent model of the proposed optical clocked D flip-flop can be verified using the highly reliable and user-friendly Opti-BPM software. The Layout of Optical clocked D flip-flop is shown in fig.4. The input data bit pattern “10011001” has been applied one by one in the form of the electrode voltage at the second electrode of the MZI1. Since, complicated backward movement of the waveguide in the Opti-BPM software, we have provided the feedback manually at the second input port of MZI2. However, the proposed layout has been simulated for the different cases and can be represented using the fig. (5)-(8).

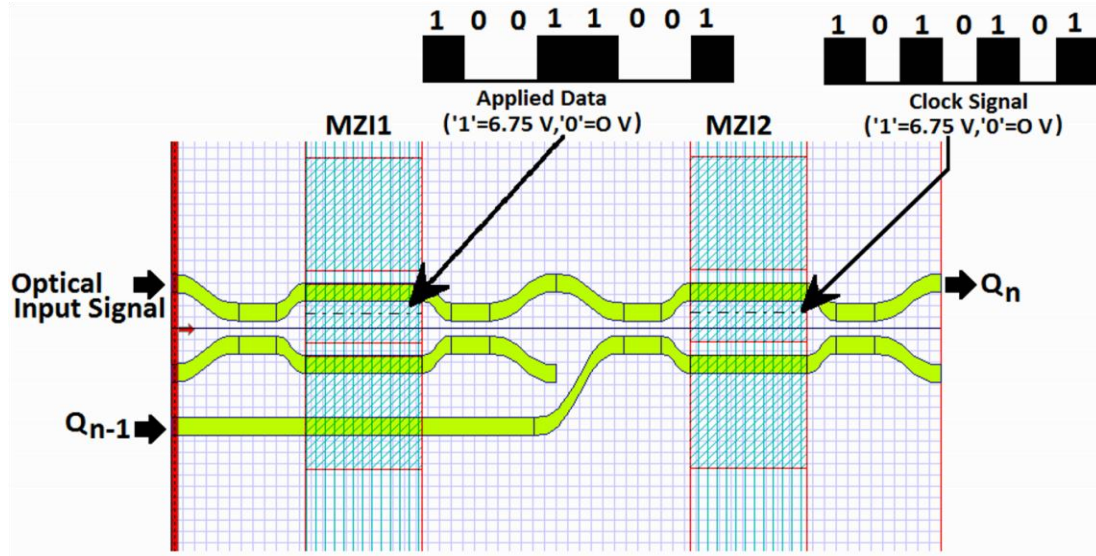


Fig. 4: Layout of all optical clocked D flip-flop

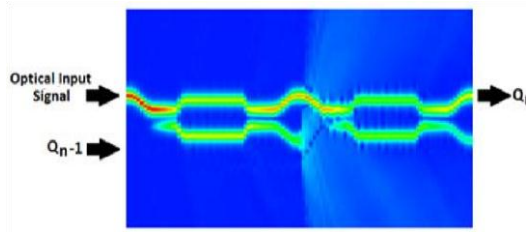


Fig. 5: clock = '1', Data bit = '1',
(Q_{n-1}) = '0', Q_n = '1'

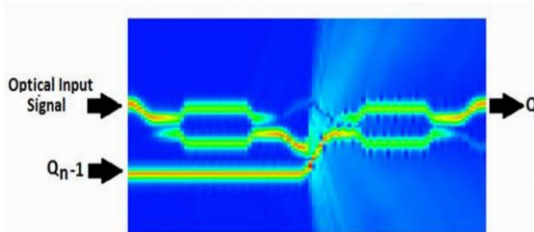


Fig. 6: clock = '0', Data bit = '0',
(Q_{n-1}) = '1', Q_n = '1'

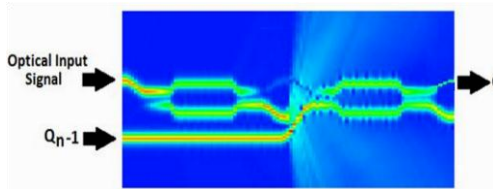


Fig. 7: clock = '1', Data bit = '0',
(Q_{n-1}) = '1', Q_n = '0'

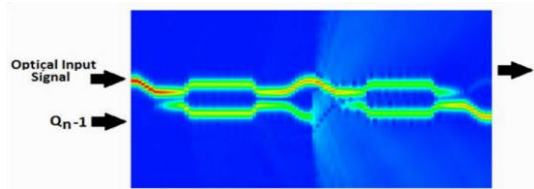


Fig. 8: clock = '0', Data bit = '1',
Feedback (Q_{n-1}) = '0', Q_n = '0'

III. DESIGN OF BARKER CODE SEQUENCE GENERATOR

Barker code is widely used in communication as an error correcting code. Due to its property of having low power, sharp auto correlation function and relatively high energy, and lower side lobes make it suitable for high accuracy and resolution in delay management.

Barker code is set of sequences x_0, \dots, x_{N-1} and they satisfy the condition

$$\sum_{i=0}^{N-1-k} x_i x_{i+k} = p(k) = \begin{cases} N & k = 0 \\ 0, \pm 1 & k = 1, 2, \dots, n - 1 \end{cases} \quad \text{Eq.7}$$

Some well-known barker code sequence and their side lobe level are shown in table 2.

Table 2. Side lobe level of some Barker code sequences

Length	Code sequences	Side Lobe Level Ratio
2	+1 -1 +1 +1	-6dB
3	+1 +1 -1	-9.5dB
4	+1 +1 -1 +1 +1 +1 +1 -1	-12dB
5	+1 +1 +1 -1 +1	-14dB
7	+1 +1 +1 -1 -1 +1 -1	-16.9dB
11	+1 +1 +1 -1 -1 -1 +1 -1 -1 +1 -1	-20.8dB
13	+1 +1 +1 +1 +1 -1 -1 +1 +1 -1 +1 -1 +1	-22.3dB

The circuit diagram of 5-Bit barker code sequence generator is shown in Fig.9. Five flip-flops are cascaded and the XOR value of the output sequence Q_3 and Q_4 is calculated and given as a feedback to the first flip-flop.

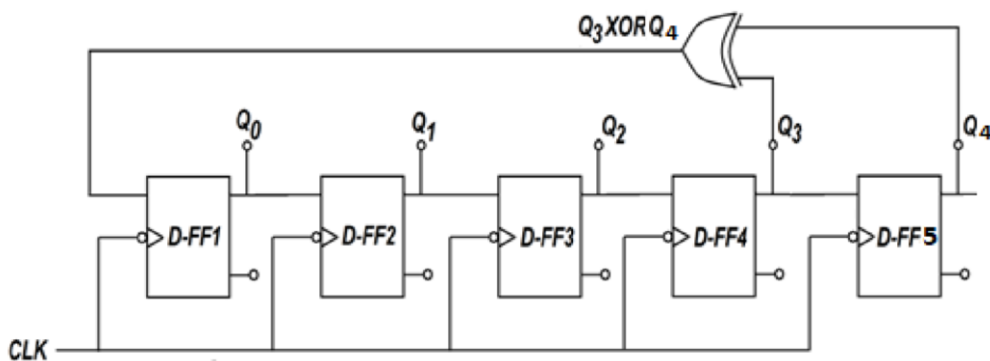


Fig. 9: Block diagram of barker code sequence generator

The Barker code sequence generator generates the 5-bit random sequence, whose patterns are completely decided by the initial bit sequence. The basic structure of 5-bit random sequence generator consists of five identical D-flip flop connected in the form of the shift registers, where the output Q_3 and Q_4 is applied to the XOR logic gate and

the output obtained from the XOR logic gate is applied to the input of the first D-flip flop. The specific arrangement of the 5 identical D flip-flop and XOR logic gate provides the 32 combinations of the random bit patterns, where the pattern completely depends upon the initial bit sequence. If we consider the initial bit pattern as $Q_0Q_1Q_2Q_3Q_4 \rightarrow 10000$, then the shifting of bit sequences provides the different bit sequence as shown in the truth table 2.

Table 2: Truth table of 5-bit Barker code sequence generator where the initial pulse is $Q_0Q_1Q_2Q_3Q_4 \rightarrow 10000$

clock	Q_0	Q_1	Q_2	Q_3	Q_4
0	0	0	0	0	0
1	1	0	0	0	0
2	0	1	0	0	0
3	0	0	1	0	0
4	1	0	0	1	0
5	0	1	0	0	1
6	1	0	1	0	0
7	1	1	0	1	0
8	0	1	1	0	1
9	0	0	1	1	0
10	1	0	0	1	1
11	1	1	0	0	1
12	1	1	1	0	0
13	1	1	1	1	0
14	1	1	1	1	1
15	0	1	1	1	1
16	0	0	1	1	1
17	0	0	0	1	1
18	1	0	0	0	1
19	1	1	0	0	0
20	0	1	1	0	0
21	1	0	1	1	0
22	1	1	0	1	1
23	1	1	1	0	1
24	0	1	1	1	0
25	1	0	1	1	1
26	0	1	0	1	1

clock	Q_0	Q_1	Q_2	Q_3	Q_4
27	1	0	1	0	1
28	0	1	0	1	0
29	0	0	1	0	1
30	0	0	0	1	0
31	0	0	0	0	1

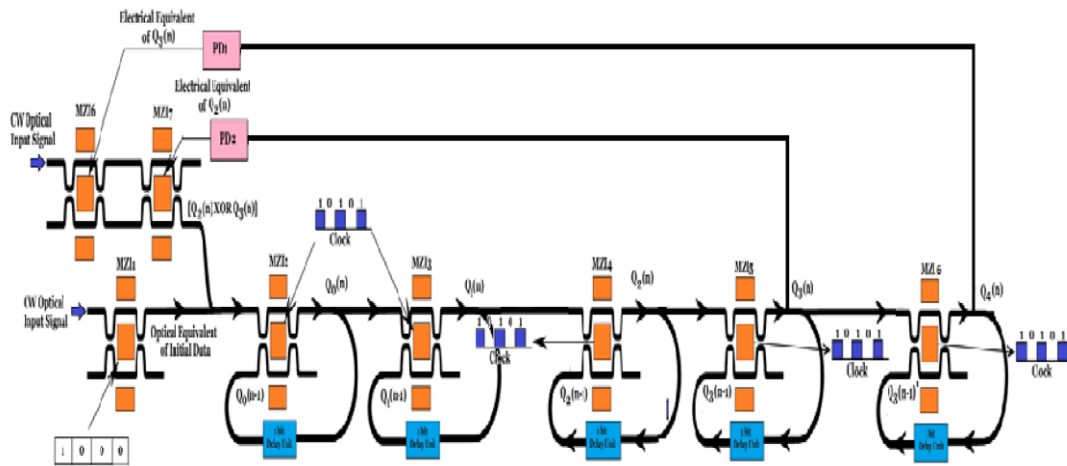


Fig.10 Proposed Circuit diagram of the barker code Sequence generator.

The fig. 10 describes the basic layout diagram of 5-bit Barker code sequence generator. The layout comprises of 8 identical of MZI structures. Basically, the MZI1 is used to convert the electrical data applied at the second electrode, into the form of the optical pulses. The data bits are applied in such a manner that, the initial set of optical output ($Q_0Q_1Q_2Q_3Q_4$) \rightarrow 10000. MZI2-MZI6 behaves as the feedback path and 1-bit delay unit assisted optical clocked D flip-flop, which is connected in a series manner, where the output of each flip-flop behaves as the input of next optical clocked D-flip flop. The specific arrangement of MZI7 and MZI8 computes the optical signal equivalent to $Q_2 XOR Q_3$. MZI2-MZI6 is driven by the same clock signal, where the clock signal is applied at the second electrode of MZI2-MZI6. The CW optical input signal is applied at the input port of MZI1 and MZI6. The electrical equivalent of Q_2 and Q_3 is computed using the photo-detector and applied at the second electrode of MZI6 and MZI7. The specific arrangement of MZI6 and MZI7 provides the optical signal equivalent to $Q_2 XOR Q_3$. The optical signal equivalent to $Q_2 XOR Q_3$ is applied to the input terminal of the MZI2, which behaves as the input bit for the further clock signals. Finally, the data bits obtained from data the throughput port of MZI2, MZI3, MZI4, MZI5, and MZI6.

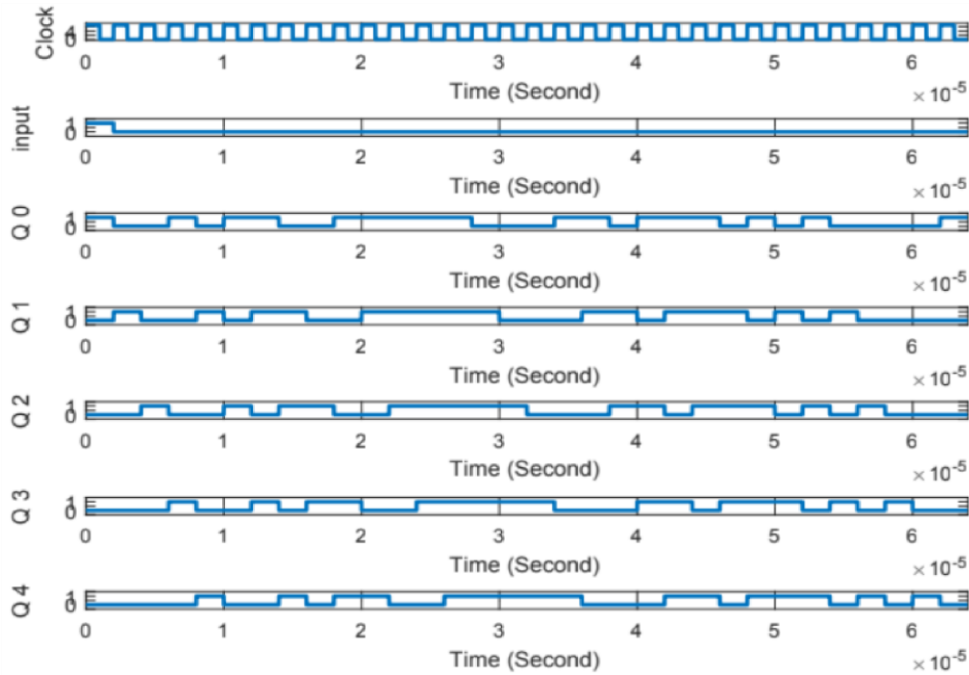


Fig.11: Simulation result of proposed barker code Sequence generator circuit

Figure 11 shows the MATLAB simulation result obtained from the proposed mechanism. The First and second row represents the presence of clock signal and initial data bit pattern. Third, fourth, fifth and sixth row represents the variation of Q_0 , Q_1 , Q_2 , Q_3 and Q_4 , respectively. The appropriateness of MATLAB simulation plot can be verified using the table 2. However, the proposed mechanism is also implemented using the Opti- BPM software.

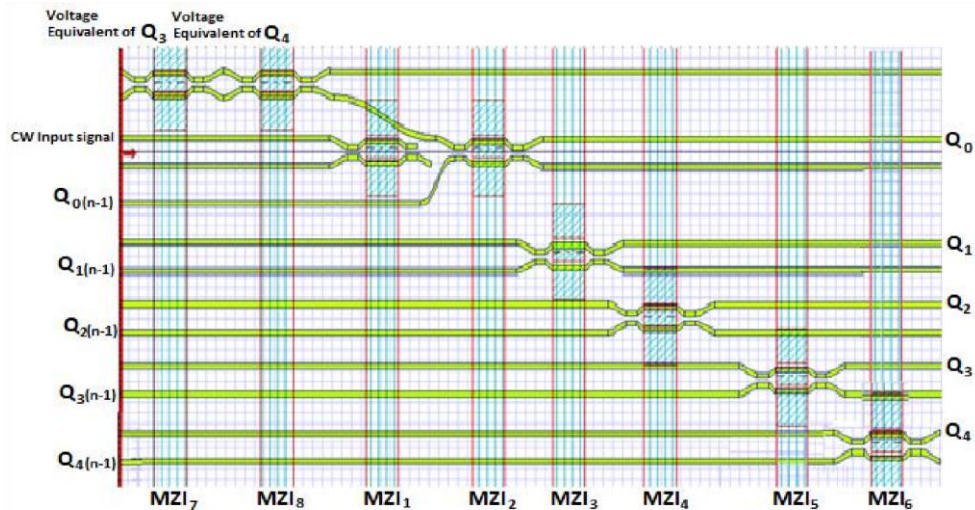


Fig. 12: Layout diagram of proposed all optical 5-bit barker code sequence generator using the Mach-Zehnder interferometer structure

The fig. 12 shows the basic layout diagram of 5- Bit barker code sequence generator using the electro-optic effect based Mach-Zehnder interferometer structure. The specific arrangement of 7 identical MZIs is simulated using Opti -BPM software. CW optical input signal is applied at the input port of the MZI1 and MZI6. Initially, throughput port of MZI2. MZI3, MZI4, MZI5, and MZI6 are set as $Q_0 \rightarrow 1, Q_1 \rightarrow 0, Q_2 \rightarrow 0, Q_3 \rightarrow 0$ and $Q_4 \rightarrow 0$, respectively. As the backward propagation of optical signal could not be possible in the Opti-BPM, hence the upper input port of the MZI3, MZI4, MZI5 and MZI6 is given manually as $Q_0(n), Q_1(n), Q_2(n)Q_3(n)$, respectively. In a similar manner, the previous output data have been applied in the form of the feedback. The manual feedback signal has been applied as $Q_0(n - 1), Q_1(n - 1), Q_2(n - 1), Q_3(n - 1)$ and $Q_4(n - 1)$ at the second input port of the MZI2, MZI3, MZI4, MZI5 and MZI6. Now, after the initial stage, the optical equivalent of

$Q_3(n) XOR Q_4(n)$ obtained from the second output port, is applied as the input of MZI1. The Proposed layout diagram is simulated for the different clock pulses and output is observed, the result of the 22nd clock pulse is shown in figure 13.

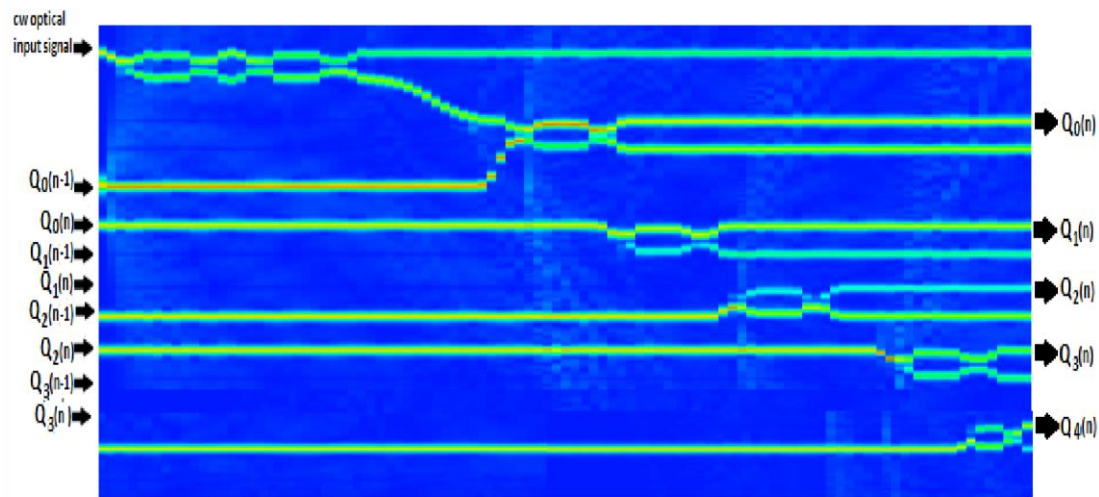


Fig.13. Simulated result of the 22nd clock pulse, $Q_0 \rightarrow 1, Q_1 \rightarrow 1, Q_2 \rightarrow 0, Q_3 \rightarrow 1$ and $Q_4 \rightarrow 1$

IV. CONCLUSION

In this paper, we have discussed future aspects of optical wireless communication.

We investigated a barker code generator in optical domain composed of ElectroOptic effect based MZI Structure. Initially the proposed device is numerically evaluated the operation performance and feasibility of the proposed device, and finally, the layout diagram is simulated using Opti-BPM, analytical and simulated results are discussed. The implementation of the barker code in the optical wireless domain can be a completely new technology. Moreover, the implementation in optical domain can make our system more efficient and free from electromagnetic interference.

REFERENCES

- [1] A. H. Gnauck, P. J. Winzer: 'Optical phase-shift-keyed transmission', *J. Light w. Technol.*, 2005, 23, (1), pp. 115–130
- [2] C. G. Lee, Y. J. Kim, C. S. Park, et al., 'Experimental demonstration of 10-Gb/s data format conversion between NRZ and RZ using SOA-Loop-Mirror', *J. Lightw. Technol.*, 2005, 23, (2), pp. 834–841
- [3] L. Xu, B. C. Wang, V. Baby, I. Glesk, P. R. Prucnal, 'All-optical data format conversion between RZ and NRZ based on a Mach-Zehnder interferometric wavelength converter', 2003, *IEEE Photon. Technol. Lett.*, 15, (2), pp. 308–310
- [4] N. Pleros¹, P. Zakyntinos¹, A. Poustie², et al.: 'Optical signal processing using integrated multi-element SOA-MZI switch arrays for packet switching' 2007, 1, (3), pp. 120 – 126
- [5] Z. Ghassemlooy, W.P. Ng, H. Le-Minh, 'BER performance analysis of 100 and 200Gbit/s optical OTDM node using symmetric Zehnder switches', *IEE Proc.-Circuits Devices Syst.*, 2006, 153, (4), pp. 361 – 369
- [6] J. Proesel, et al., "25Gb/s 3.6pJ/b and 15Gb/s 1.37pJ/b VCSEL-based optical links in 90nm CMOS," *ISSCC Dig. Tech. Papers*, pp. 418-420, Feb. 2012.
- [7] Qiang Wang, Guanghao Zhu, et al., "Study of All-Optical XOR Using Mach-Zehnder Interferometer and Differential Scheme", *IEEE JOURNAL OF QUANTUM ELECTRONICS*, VOL. 40, NO. 6, JUNE 2004.
- [8] Tanay Chattopadhyaya, Jitendra Nath Roy, "Design of SOA-MZI based all-optical programmable logic device (PLD)", *Optics Communications* 283 (2010) 2506–2517
- [9] H.S. Chung, R. Inohara, K. Nishimura and M. Usami, "All-optical multi-wavelength conversion of 10 Gbit/s NRZ=RZ signals based on SOA-MZI for WDM multicasting" *ELECTRONICS LETTERS* 31st March 2005 Vol. 41 No. 7.
- [10] D. Petrantonakis, G.T. Kanellos, et al., "A 40 Gb/s 3R Burst Mode Receiver with 4 integrated MZI switches", *Optical Society of America*, 2006
- [11] S. K. Raghuvanshi, Ajay Kumar, Santosh Kumar, "1 × 4 Signal Router Using 3 Mach-Zehnder Interferometers", *Optical Engineering (SPIE)*, 52(3), 035002 (2013).
- [12] L. F. Stokes, M. Chodorow, H. J. Shaw, "All single mode fiber resonator," *Opt. Lett.* 7(6), 288-290 (1982).
- [13] B. Moslehi, "Fiber-optic lattice signal processing," *Proc. IEEE*, 72(7), 909-930 (1984). [14] K. P. Jackson, G. Xiao, H. J. Shaw, "Coherent optical fiber delay line processor," *Electron. Lett.*, 22(5), 1335 – 1337 (1986).
- [15] Sanjeev Kumar Raghuvanshi, Ajay Kumar, Nan K Chen, "Implementation of sequential logic circuit using the Mach-Zehnder interferometer based on

- electro-optic effect,” *Optics Communications*(Elsevier), 333, 193-208(2014).
- [16] Ajay Kumar, Santosh Kumar, S. K. Raghuwanshi, “Implementation of XOR/XNOR and AND logic gates using Mach-Zehnder interferometers,” *Optik* (Elsevier), 125, 5764 – 5767(2014).
- [17] Ajay Kumar, Sanjeev Kumar Raghuwanshi, “Implementation of optical gray code converter and even parity checker using the electro-optic effect in the Mach-Zehnder interferometer structure” *Optical and Quantum Electronics* (Springer) DOI 10.1007/s11082-014-0087-9.
- [18] Ajay Kumar, Santosh Kumar, S. K. Raghuwanshi, “Implementation of full adder and full-subtractor based on electro-optic effect in Mach-Zehnder interferometers,” *Optics Communications* (Elsevier), 324, 93-107(2014).

